# Raman study of surface optical phonons in ZnO(Co) nanoparticles prepared by calcinations method

B. HADŽIĆ[a], N. ROMČEVIĆ[a], M. ROMČEVIĆ[a], I. KURYLISZYN-KUDELSKA[b], W. DOBROWOLSKI[b], M. GILIĆ[a], M. PETROVIĆ DAMJANOVIĆ[a], J. TRAJIĆ[a], U. NARKIEWICZ[c], D. SIBERA[c]
[a]*Institute of Physics, University of Belgrade, Pregrevica 118, 11 080 Belgrade, Serbia*
[b]*Institute of Physics, Polish Academy of Science, al. Lotnikow 32/46, 02-668 Warszawa, Poland.*
[c]*Szczecin University of Tehnology, Institute of Chemical and Environment Engineering, Pulaskiego 10, 70-322 Szczecin, Poland*

In Raman scattering spectra of nanocrystaline samples ZnO(Co), surface optical phonons (SOP) were observed in the range of 496 – 546 $cm^{-1}$. With X - ray diffraction measurements were determined the phase composition of the samples (ZnO, $Co_3O_4$) and the mean crystalline size (14-156 nm) where 53% of samples have mean crystalline size between 14 and 30 nm, 24% between 40 and 60nm, 17% larger than 100 nm and 6% have 80 nm. From this measurement becomes obvious the change of position of SOP modes with crystalline size and change of intensity of SOP modes with change of CoO concentration of doping element.

(Received October 10, 2013; accepted May 15, 2014)

*Keywords*: Nanostructured materials, Optical properties, Light absorption and reflection

## 1. Introduction

The synthesis and the properties of nanoscale inorganic materials has been attracted great interest, especially nanostructures made of ZnO and ZnO-related compounds due to their large expected spectra of applications. Some of them are in the quality of transparent conducting electrodes for solar cells and flat panel displays, in spintronic devices, transparent ultraviolet protection films and low-voltage and short-wavelength electro-optical devices [1,2].

It has been observed that ZnO is most promising host semiconductor material for high temperature ferromagnetism, because it exhibits ferromagnetism when it is doped with majority of the transition metals such as Co, Ni, Cr, Fe, V [3].

Raman scattering has been a method of choice for many studies of vibrational properties of ZnO, for bulk materials, thin films and nanostructure samples, both pure and doped due to its characteristics of an ideal sensitive, non-destructive tool. It permits obtaining information about the sample quality, presence of impurities and their position in host lattice as well as information about phonon lifetimes and isotopic effects [4, 5]. In ZnO and ZnO-related compounds with Raman scattering has been studied local atomic arraignment, dopant incorporation, electron-phonon coupling, multi phonon process, influence of annealing process, temperature dependence of Raman modes and others [6-11].

For nanostructures of ZnO the appearance of surface optical phonon (SOP) modes in Raman spectra is expected because of their large surface-to-volume ratio. This is the reason why the state of surface atoms have important role in determining their properties. Surface modes are only modes that persist when dimensions becomes extremely small. With this we can say that SOP modes are Raman forbidden modes whose presence is related to loss of long-range order and symmetry breakdown in ZnO shell [12,13]. All this can be found in many papers predicted theoretically and/or detected experimentally for ZnO nanostructures [12].

The aim of this work is to study samples characteristics, by applying micro-Raman spectroscopy to study the Co ion position in ZnO lattice, the formation of existing phases, presence of SOP modes and quality of the samples in dependence of CoO concentration.

## 2. Samples and characterization

The nanocrystalline samples of ZnO doped with CoO were obtained using of the coprecipitation-calcination method. In this method a mixture of cobalt and zinc hydroxides was obtained by addition of an ammonia solution or 2M solution of KOH to the 20% solution of a proper amount of $Zn(NO_3)*6H_2O$ and $Co(NO_3)*4H_2O$ in water. Next, the obtained hydroxides were filtered, dried at 70 °C and calcined at 300 °C during one hour. Nanopowders obtained on this way were pressed into indium panel.

This method allowed obtaining the series of nanosized ZnO samples with nominal concentration of CoO from 5% to 95%. In this paper we present the results of micro-Raman spectroscopy for all obtained samples as well as the changes of intensity of modes with concentration of CoO.

Firstly, the quality of samples was investigated by examining their morphology with scanning electron microscope (SEM). In SEM images for lower concentration of CoO can be easily distinguish two types of particles, one bigger than 100 nm, which belongs to ZnO phase and other much smaller, that belongs to $Co_3O_4$ phase. With CoO concentration increase the size of particles becomes similar, while further increase to the highest level of CoO concentration leads to dominance of smaller particles that belongs to $Co_3O_4$ phase.

*Table 1. XRD analysis results for samples prepared by calcinations method. The identified crystalline phases and mean crystalline size d has been determined by use of Scherrer's formula.*

| | d [nm] ZnO phase | d [nm] $Co_3O_4$ phase |
|---|---|---|
| 5 wt.% | 156 | 55 |
| 10 wt.% | 118 | 50 |
| 20 wt.% | 57 | 21 |
| 30 wt.% | 101 | 30 |
| 40 wt.% | 80 | 17 |
| 50 wt.% | 43 | 21 |
| 60 wt.% | - | 14 |
| 70 wt.% | - | 15 |
| 80 wt.% | - | 21 |
| 90 wt.% | - | 25 |
| 95 wt.% | - | 20 |

Secondly, we used X-ray diffraction (XRD) ($Co_{K\alpha}$ radiation, X'Pert Philips) to determine the phase composition of samples. In our samples, prepared by calcinations method, XRD analysis revealed the presence of crystalline phases of spinel structure $Co_3O_4$ (ICSD: 80-1540) and hexagonal ZnO. XRD parameters obtained this way allowed us, using Scherrer's formula [14], to determine a mean crystalline size in these samples. The mean crystalline size d, in our samples prepared by calcinations method, are between 14 and 55 nm for $Co_3O_4$ phases and from 43 to 156 nm for ZnO phases. These results, the phase composition and the mean crystalline size are gathered in Table 1.

Previously obtained results indicated that for ours samples, prepared by calcinations method, crystalline size of ZnO generally decreases with increasing of CoO, while the crystalline size of second phase $Co_3O_4$ does not have monotonous dependence. Relative change of crystalline size of ZnO phase is bigger than the corresponding change of $Co_3O_4$ phase. The presence of ZnO phase has been registered in samples doped with 60 % of CoO and more, but the results obtained for their crystallite size are unreliable, that's why it hasn't been shown in Table 1.

In this paper we present result of our investigation for all obtained samples. Beside these two phases, no others have been observed.

## 3. Surface optical phonons

Here we will give a brief concept of surface optical phonons (SOP). Reduction of the particles dimensions to nanoscale, as in our case, and presence of imperfections, impurity and others, results in breakdown of phonon momentum selection rules. That is why some new forbidden vibration modes whose phonons have $l \neq 0$ can contribute to Raman scattering [15-17, 6]. Also we can mention that SOP modes appear in samples which particles size is smaller then the wavelength of incident laser beam and that these modes arise in polar crystals [13]. In the literature can be found the dielectric function for the case of polar semi-insulating semiconductor [see for example Ref.15. and literature cited there], many mixing models for the effective dielectric permittivity [18], as well as Maxwell-Garnet mixing rule [19,20]. However the Maxwell-Garnet approximation is only valid for small volume fraction of inclusions and is not appropriate in our case. That's why we will be focused on Bruggerman formula and it mixing rule [21-23] which is much more appropriate in our case. In Bruggeman model there is no exist restrictions for volume fraction, and that is why it is suitable for high concentration of inclusions. The effective dielectric function according to the Bruggeman mixing rule is given by:

$$(1-f)\frac{\varepsilon_1-\varepsilon_{eff}}{\varepsilon_{eff}+g\left(\varepsilon_1-\varepsilon_{eff}\right)}+f\frac{\varepsilon_2-\varepsilon_{eff}}{\varepsilon_{eff}+g\left(\varepsilon_2-\varepsilon_{eff}\right)}=0 \qquad (1)$$

where, g is a geometric factor who depends on the shape of the inclusions. In the case of two-dimensional circles g=1/2, while for the three dimensional spherical particles g=1/3.

In our samples nanoparticles are clusterized, they occupy a significant volume and are not well-separated in air, that's why they satisfy the Bruggeman formula conditions with g=1/3 appliance.

For ZnO nanoparticles, in a region of appearance of SOPs, we have two phonons $\omega_{A_{1LO}}=577\,\mathrm{cm}^{-1}$, $\omega_{A_{1TO}}=379\,\mathrm{cm}^{-1}$, $\omega_{E_{1TO}}=410\,\mathrm{cm}^{-1}$, $\omega_{E_{1LO}}=592\,\mathrm{cm}^{-1}$, with dielectric permittivity $\varepsilon_\infty=3,7$ [24-26]. In our case we can neglect influence of the plasmon-phonon interaction because of low free carriers concentration and low mobility. Nanoparticles of our samples are randomly distributed in space and accordingly to the incident light. Having in mind that the $A_1$ symmetry phonon is registered in Raman spectra, while there is no $E_1$ symmetry phonon,

this can indicate that the $E_1$ symmetry phonon participate in SOP creation. Existence of $A_1$ symmetry phonon and non existence of $E_1$ symmetry phonon will be shown later. The excitation of extraordinary phonons results in Raman intensity given with:

$$I \sim \mathrm{Im}\left(\frac{-1}{\varepsilon_{eff}}\right) \tag{2}$$

This type of calculation predicts appearance of one asymmetric peak in the area of Bruggerman formula applicability with wavenumbers below $\omega_{E1}(LO)$. Obtained experimental spectra of ZnO doped with CoO nanopowders shows good agreement with this calculations. The great difference in the intensity and line shape of simulated SOP modes, as we shall see later, is mainly the results of variation in main volume fraction and damping rate.

## 4. Results and discussion

The micro-Raman spectra were taken in the backscattering configuration and analyzed using Jobin Yvon T64000 spectrometer, equipped with nitrogen cooled charge-coupled-device detector. As excitation source we used the 514.5 nm line of an Ar-iron laser. The measurements were performed at 20 mW laser power.

For analysis of Raman spectra we have assumed that all phonon lines are of Lorentzian type which is one of common type of lines for this kind of analysis, other common type of line is Gaussian [27]. We used equations 1 and 2 to calculate SOP lines, with $\varepsilon_1 = 1$.

In Figs. 1 and 2 are presented obtained Raman spectra for all samples of nanocrystaline ZnO doped with CoO prepared by calcinations method. In these samples, as we already have mentioned, with XRD analysis only nanoparticles of ZnO and $Co_3O_4$ are registered. For analysis of vibrational properties of nanoparticles it is crucial to understand vibration properties of bulk material. That's why we start analysis of obtained Raman spectra with brief report about structural and vibration properties of all potentially present phases in the samples. We expect that bulk modes will be shifted and broadening as a consequence of miniaturization.

ZnO, basic material in our samples, is a semiconductor with a wurtzite crystal structure. With four atoms per primitive cell, this hexagonal structure belongs to $C_{6v}^4$ space group and all atoms occupy $C_{3v}$ sites. As it has been seen many times [28,29] ZnO have four Raman active modes ($A_1$, $E_1$ and $2E_2$) where $A_1$ and $E_1$ are polar modes and they split into transverse (TO) and longitudinal (LO) phonons. This TO and LO phonons have different frequencies due to macroscopic electric fields (associated with the LO phonons) and anisotropy caused by the short-range interatomic forces. The TO-LO splitting is larger than the $A_1$-$E_1$ splitting due to anisotropy caused by dominances of electrostatic forces in the short-range force region. In bulk ZnO $A_1$ atoms move parallel to the c-axis and $E_1$ perpendicular to c-axis for the lattice vibration. Often, two nonpolar Raman active modes, are assigned with $E_2^{(1)}$(low) and $E_2^{(2)}$(high). Whit this in mind we gathered most typical frequencies and assignation of ZnO Raman active modes in Table 2 [28,29].

*Table 2. Frequencies and assignation of most typical Raman active modes in ZnO.*

| Frequencies for bulk ZnO [$cm^{-1}$] | Assignation of modes |
|---|---|
| 102 | $E_2^{(1)}$ (low) |
| 330 | multi phonon |
| 379 | $A_1$(TO) |
| 410 | $E_1$(TO) |
| 437 | $E_2^{(2)}$ (high) |
| 541 | $A_1$(LA) |
| 577 | $A_1$(LO) |
| 592 | $E_1$(LO) |
| 660 | multi phonon |
| 1153 | multi phonon |

*Table 3. Frequencies and assignation of Raman active modes in $Co_3O_4$.*

| Frequencies for bulk $Co_3O_4$ [$cm^{-1}$] | Assignation of modes |
|---|---|
| 194,4 | $F_{2g}$ |
| 482,4 | $E_g$ |
| 521,6 | $F_{2g}$ |
| 618,4 | $F_{2g}$ |
| 691,0 | $A_{1g}$ |

$Co_3O_4$ belongs to $O_h^7$ space group and crystallizes in the normal spinal structure $Co^{2+}(Co^{3+})_2O_4^{2-}$ where $Co^{2+}$ and $Co^{3+}$ are placed at tetrahedral and octahedral sites, respectively. Its primitive unit cell contains 14 atoms and it has 5 Raman active modes ($A_{1g}$, $E_g$ and three $F_{2g}$) [30]. In Table 3 we gathered frequencies and assignation of Raman active $Co_3O_4$ modes presented in this paper [30].

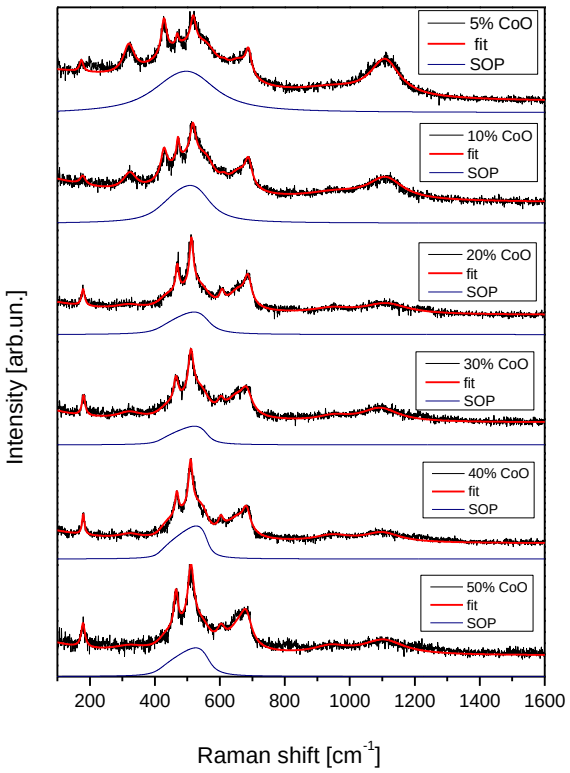


*Fig. 1. Fitted Raman spectra of nanocrystaline ZnO doped with CoO from 5% to 50 %; fitted SOP modes are marked with blue solid lines.*

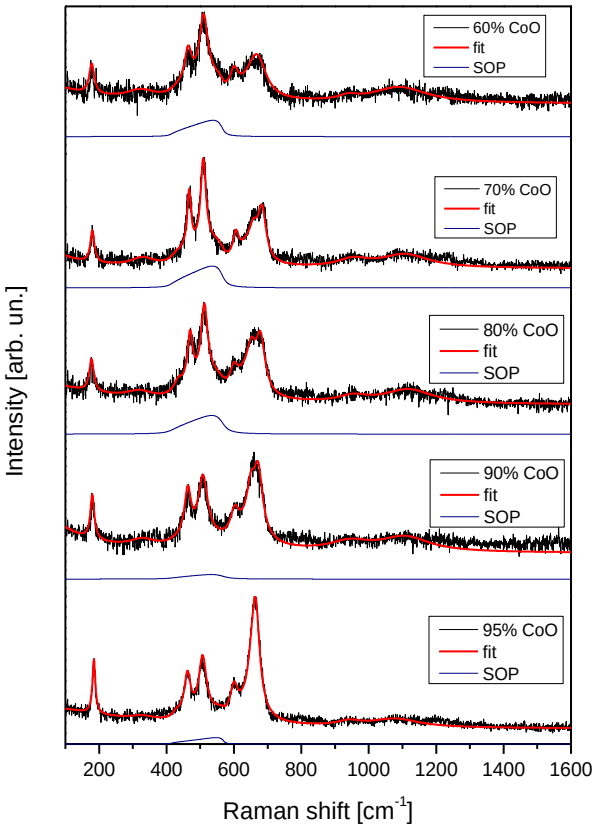


*Fig. 2. Fitted Raman spectra of nanocrystaline ZnO doped with CoO from 60% to 95%; fitted SOP modes are marked with blue solid lines.*

In Figs. 1 and 2 are given all Raman spectra of samples obtained by calcination method, in Fig. 1 for the samples doped from 5% CoO till 50% CoO while on the Fig. 2 are given Raman spectra of samples doped from 60% CoO to 95% CoO. On these spectra are evident existence of single and multi phonons modes characteristic for ZnO, such as 379 $cm^{-1}$ ($A_1$(TO)), 437 $cm^{-1}$ ($E_2^{(2)}$), 577 $cm^{-1}$ ($A_1$(LO)), and multi phonons at 330, 660 and ~1110 $cm^{-1}$. From all these modes characteristic for ZnO one is the most obvious. That is the mode at 437 $cm^{-1}$. Its sharp peak is clearly visible on Raman spectra for smaller concentration of doping element (CoO), and with increase of CoO concentration its intensity decreases. All others phonon modes of ZnO behave on the same way as the mode at 437 $cm^{-1}$. Beside these modes characteristic for ZnO in these samples we also notice existence of typical modes for $Co_3O_4$ phase, such as 194 $cm^{-1}$ ($F_{2g}$), 482 $cm^{-1}$ ($E_g$), 521 $cm^{-1}$ ($F_{2g}$), 618 $cm^{-1}$ ($F_{2g}$) and 691 $cm^{-1}$ ($A_{1g}$). Opposite from ZnO modes, $Co_3O_4$ modes increase their intensity with increase of concentration of CoO. The most evident $Co_3O_4$ modes in these spectra are 482 $cm^{-1}$, 521 $cm^{-1}$ and 691 $cm^{-1}$. Here we need to emphasize that position of peak centers are on lower frequencies, which is a consequence of nanosized structure of this samples but in good agreement with earlier reported Raman frequencies for bulk crystals, gather in work of M. Bouchard at all [31]. In all this spectra it can be noticed the changes of spectra with concentration of CoO. These results of Raman spectroscopy are in good agreement with previously done XRD analysis. Apart all modes that we have mentioned, in each and every Raman spectra, it is also evident the existence of additional structure. This structure is SOP mode and they have been shown on each spectrum. These SOP modes, as we already mentioned, originate from ZnO nanoparticles due to nanosize structure of samples. Change of characteristic SOP modes with concentration of doping element (CoO) is shown in Fig. 3.

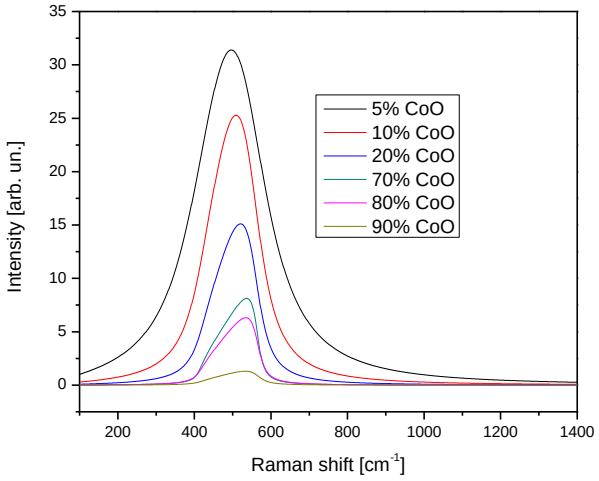


*Fig. 3. Change of characteristic SOP modes with concentration of dopant (CoO).*

From this figure it is clearly visible that the change in position of SOP modes directly follows the decrease of crystalline size of ZnO. Along this, in Fig. 3 we can notice

that intensity of SOP modes decreases with increase of doping element; in our case that is CoO. This change of intensity of SOP modes is similar to the change of intensity of ZnO modes and opposite to the change of intensity of $Co_3O_4$ modes, which is one more proof that SOP modes originate from ZnO.

## 5. Conclusion

Morphology of investigated samples was firstly examined using SEM where we found an evident existence of particles with different size, smaller particles which belong to $Co_3O_4$ phase, while bigger belong to ZnO phase.

The phase composition of the samples was determined by X-ray diffraction, where the crystalline phases of ZnO and $Co_3O_4$ were identified.

In the Raman spectra of all prepared samples there are evident existence of single and multi phonon modes characteristic for ZnO. Beside these modes we also noticed existence of typical modes for $Co_3O_4$ phase. Apart from all modes that we have mention, in every Raman spectra, is also evident the existence of surface optical phonon (SOP) mode. We have investigated characteristics of SOP modes and notice that the change in their position directly follows the change of crystalline size. Along this, intensity of ZnO and SOP modes decreases with increase of CoO concentration, while intensity of $Co_3O_4$ modes increases with increase of CoO concentration.

**Acknowledgements**

This work was supported under the Agreement of Scientific Collaboration between Polish Academy of Science and Serbian Academy of Sciences and Arts. The work in Serbia was supported by Serbian Ministry of Education and Science (Project 45003) and in Poland by National Science Center granted under decision No. DEC-2011/01/B/ST5/06602.

## References

[1] Y. Chen, D.M. Bagnall, H. Koh, K. Park, K. Higara, Z. Zhu and T. Yao, J. Appl. Phys., **84,** 3912 (1988).
[2] J. Nemeth, G. Rodriguez-Gattorno, A. Diaz and I. Dekany, Langmuir, **20,** 2855 (2004).
[3] J. M. D. Coey, M. Venkatesan and C.B. Fitzgerald, Nat. Mater., **4**, 173 (2005).
[4] T. Dietl, Acta Phys. Pol., **A 111**, 27 (2007).
[5] C. Sudakar, J. S. Thakur, G. Lawes, R. Naik, V. M. Naik, Phys. Rev., **B 75**, 054423 (2007).
[6] R. Cuscó, E. Alarcón-Lladó, J. Ibáñez, L. Artús, J. Jiménez, B. Wang, M. J. Callahan, Phys. Rev., **B 75**, 165202 (2007).
[7] Y. Liu, J. L. MacManus-Drisoll, Appl. Phys. Letters, **94,** 022503 (2009).
[8] J. Xu, W. Ji, X. B. Wang, H. Shu, Z. X. Shen, S. H. Tang, J. Raman Spectrosc., **29,** 613 (1998).
[9] H. Zeng, W. Cai, B. Cao, J. Hu, Y. Li, P. Liu, Appl. Phys. Lett., **88,** 181905 (2006)
[10] N. Romčević, R. Kostić, B. Hadžić, M. Romčević, I. Kuryliszin-Kudelska, W. Dobrowolski, U. Narkievicz, D. Sibera, Journal of Alloys and Compounds, **507,** 386 (2010).
[11] M. Millot, J. Gonzalez, I. Molina, B. Salas, Z. Golacki, J.M. Broto, H. Rakoto, M. Gorian, JALLCOM, **423**, 224 (2006).
[12] R. P. Wang, G. Xu, P. Jin, Phys. Rev., **B 69,** 113303 (2004).
[13] R.Y. Sato-Berrú, A. Vázquez-Olmos, A. L. Fernández-Osorio, S. Sotres-Martínez, J. Raman Spectrosc., **38,** 1073 (2007).
[14] P.-M. Chassaing, F. Demangeot, V. Paillard, A. Zwick, N. Combe, C. Pages, M. L. Kahn, A. Maisonnat, B. Chaudret, Phys. Rev., B **77**, 153306 (2008).
[15] G. Irmer, J. Raman Spectrosc., **38,** 634 (2007).
[16] A.L. Patterson, Phys. Rev., **56,** 978 (1939).
[17] H. Zeng, W. Cai, B. Cao, J. Hu, Y. Li, P. Liu, Appl. Phys. Lett., **88**, 181905 (2006).
[18] A. Ghosh, R.N.P. Choudhary, J. Phys. D: Appl. Phys., **42**, 075416 (2009).
[19] F. Friedrich, N.H. Nickel, Appl. Phys. Lett., **91**, 111903 (2007).
[20] K. Karkkainen, A. Saviola, K. Nikoskinen, IEEE Transaction on geosciences and remote sensors, **39**(5), 1013 (2001).
[21] J. C. M. Garnett, Trans. R. Soc., **CCIII**, 385 (1904).
[22] A. Saviola, I. Lindell, Dielectric Properties of Heterogeneous Materials, PIER 6 Progres in Electromagnetic Research, A. Priou, Ed. Amsterdam, The Netherlands: Elsevier (1992) 101.
[23] D.A.G. Bruggeman, Ann. Phys., **24**(5), 636 (1935).
[24] J. Saarinen, E. M. Vartiainen, K. Peiponen, Optical Rewiew, **10**(2), 115 (2003).
[25] X. C. Zeng, D. J. Bergman, P. M. Hui, D. Stroud, Phys, Rev., B **38,** 10970 (1988).
[26] J.,D. Ye, S. Tripathy, F.,F. Ren, X.,W. Sun, G.,Q. Lo and K.,L. Teo, Appl. Phys. Lett., **94,** 011913 (2009).
[27] I. M. Tiginyanu, A. Sarua, G. Irmer, J. Monecke, S.M. Hubbard, D. Pavlidis, V. Valiaev, Phys. Rev., B **64,** (2333172001).
[28] M. Šćepanović, M. Grujić-Brojčin, K. Vojisavljević, S. Bernik and T. Srećković, J. Raman Spectrosc., **41,** 914 (2010).
[29] H. Idink, V. Srikanth, W. B. White, E.C. Subbarao, J. Appl. Phys., **76**, 1819 (1994).
[30] N. Ashkenov, B. N. Mbenkum, C. Bundesmann, V. Riede, M. Lorenz, D. Spemann, E. M. Kaidashev, A. Kasic, M. Shubert, M. Grundmann, J. Appl. Phys., **93**, 126 (2003).
[31] E. F. Venger, A. V. Melnichuk, L. Lu Melnichuk, Yu A. Pasechuk, Phys. Stat. solidi, B **188,** 823 (1995).
[32] V. G. Hadjiev, M. N. Iliev, I. V. Vegilov, J. Phys. C: Solid State Phys., **L199,** 21 (1988).
[33] M. Bouchard, A. Gambardella, J. Raman Spectrosc., **41**, 1477 (2010).

*Corresponding author: romcevi@ipb.ac.rs